An Evaluation of Recent Higher-order Bounded Convection Schemes

Seok Ki Choi* and Yong Bum Lee*

최근의 고차 유계 대류항 처리법의 평가

최 석 기 • 이 용 범

이 논문은 최근에 개발된 네가지 종류의 고차 유계 대류항 처리법인 SOUCUP, HLPA, SMARTER 그리고 COPLA 해법들을 비교 분석한다. 모든 해법들을 실제적인 공학적인 문제에의 적용을 위하여 비균일, 비직교 좌표에 공식화 하였다. 해법들의 상대적인 검증을 위하여 여러 가지 종류의 시험 문제들에 적용하여 검증하였다. 수치실험의 결과는 시험한 4종류의 해법들이 유계성을 만족하고 고차 해법의 정확도를 유지하는 것으로 나타났다. HLPA, SMARTER와 COPLA 해법들은 거의 같은 정도의 해의 정확성을 보였으며, SCOCUP 해법은 조금 부정확한 것으로 나타났다.

Keywords: CFD (전산유체역학), Convection Scheme (대류항 처리법), Higher-order Bounded Scheme (고차 유계 해법)

1. Introduction

Development of an efficient convection scheme which is simple to implement but is free of false diffusion has been one of the major tasks for the computational fluid dynamicists over the last two decades. The classical lower-order schemes such as the upwind scheme, the hybrid central/upwind scheme and the power-law scheme[1] are unconditionally bounded and highly stable but highly diffusive when the flow direction is skewed relative to the grid lines. A simple remedy to overcome the false diffusion is to use a fine enough grid. However, such a practice is not practical due to the requirement of excessive computer storage and computational efforts, especially in the complex three-dimensional flow calculations.

Considerable efforts have been made toward the development of the improved differencing schemes, mainly in two directions. One is raising the order of the scheme and the other is taking into account the multidimensional nature of flow. The QUICK(Quadratic Upstream Interpolation for Convective Kinematics) scheme[2] and the second-order upwind scheme[3] belong to the former approach and the skew-upwind scheme[4] the latter. These schemes have been successful in increasing the accuracy of the solution, but all suffer from the boundedness problem, resulting in an oscillatory solution behaviour in regions of steep gradient which can lead to the numerical instability.

* Member, LMR Coolant Technology/Korea Atomic Energy Research Institute

Recently, Gaskell and Lau[5] developed a higher-order bounded scheme named SMART (Sharp and Monotonic Algorithm for Realistic Transport) employing a composite approach in which the high resolution schemes are combined with the lower-order bounded schemes. Leonard[6] also proposed a similar bounded scheme of third-order accuracy named SHARP(Simple High-Accuracy Resolution Program). These two schemes have resolved the forementioned boundedness problem without much deteriorating the accuracy of the higher-order scheme. However, numerical experiments [7] have shown that these schemes need an under-relaxation treatment at each of the control volume cell faces in order to overcome the oscillatory convergence behaviors. This deficiency leads to the increase of the computer storage requirement, which may pose a practical constraint to their use in the complex three-dimensional turbulent flow calculations.

Subsequent studies by Zhu and Rodi[8], Zhu[9], Shin and Choi[10] and Choi et al.[11] have proposed bounded convection schemes which are free of oscillatory convergence behaviors by choosing simple characteristics in the normalized variable diagram, such as piecewise-linear profile (SOUCUP: Second-Order Upwind-Central differencing-first-order UPwind), a parabolic profile(HLPA: Hybrid Linear/Parabolic Approximation), a cubic profile (SMARTER: SMART Efficiently Revised) and a combination of piecewise linear profiles (COPLA: COmbination Piecewise Linear Approximation). These schemes are very simple to implement and computationally cost effective.

The objective of the present study is a systematic comparison of above three schemes, SOUCUP, HLPA SMARTER and COPLA , in the incompressible flow calculations under highly convective conditions. All the schemes are formulated on a non- uniform, non-orthogonal grid so that they can be applicable to the practical engineering flow calculations. The relative performances among the schemes are examined through applications to the several linear and non-linear test problems. The computed results by the lower-order HYBRID scheme and by the higher-order QUICK scheme are also included for a better comparison with the existing popular schemes.

2. Mathematical formulation

2.1 Governing equations

The conservation form of transport equation for a general dependent variable ϕ in a generalized coordinate system(ξ, η) can be written as follows

$$\begin{aligned}&\frac{\partial}{\partial \xi}(\rho U\phi)+\frac{\partial}{\partial \eta}(\rho V\phi)\\&=\frac{\partial}{\partial \xi}\left[\frac{\Gamma_\phi}{J}\left(D_1^1\frac{\partial \phi}{\partial \xi}+D_2^1\frac{\partial \phi}{\partial \eta}\right)\right]\\&+\frac{\partial}{\partial \eta}\left[\frac{\Gamma_\phi}{J}\left(D_1^2\frac{\partial \phi}{\partial \xi}+D_2^2\frac{\partial \phi}{\partial \eta}\right)\right]+JS_\phi\end{aligned} \tag{1}$$

where

$$U=b_1^1u+b_2^1v,\quad V=b_1^2u+b_2^2v \tag{2}$$

and

$$\begin{aligned}&b_1^1=y_\eta,\ b_2^1=-x_\eta,\ b_1^2=-y_\xi,\ b_2^2=x_\xi\\&D_1^1=x_\eta^2+y_\eta^2,\quad D_2^2=x_\xi^2+y_\xi^2\\&D_2^1=D_1^2=-(x_\xi x_\eta+y_\xi y_\eta)\\&J=x_\xi y_\eta-x_\eta y_\xi\end{aligned} \tag{3}$$

In these equations, ρ is the density of fluid, Γ_ϕ is the diffusion coefficient of the variable ϕ, (u, v) are the Cartesian velocity components in (x, y) directions and S_ϕ denotes the source term of the variable ϕ.

2.2 Discretization of transport equations

In the finite volume approach, the general transport equation, Eq.(1), is integrated over a control volume shown in Fig.1. The resulting equation can be written as follows

$$F_e-F_w+F_n-F_s=S_\phi\,\Delta V+S_\phi^b \tag{4}$$

where F represents the total flux of ϕ across the cell face and S_ϕ^b is the sum of the non-orthogonal diffusion terms. The total flux at the west face, for example, can be written as follows with the diffusion term approximated by the central differencing scheme.

$$F_w = C_w\phi_w - D_w(\phi_P - \phi_W) \tag{5}$$

where

$$C_w = (\rho U)_w, \quad D_w = \left(\frac{\Gamma_\phi}{J} D_1^1\right) \tag{6}$$

The evaluation of ϕ_w plays a key role in determining the accuracy and the stability of numerical solutions. For example, the ϕ_w is evaluated as follows when one uses the first-order upwind scheme

$$\phi_w = U_w^+ \phi_W + U_w^- \phi_F \tag{7}$$

where U_w^+ and U_w^- are the indicators of the local velocity direction such that

$$\begin{aligned} U_w^+ &= 0.5\,(1 + |U_w|/U_w), \\ U_w^- &= 1 - U_w^+ \quad (U_w \neq 0) \end{aligned} \tag{8}$$

Incorporation of Eq.(7) and Eq.(5) and similar expressions for the other cell faces leads to following general difference equation

$$A_P\phi_P = A_E\phi_E + A_W\phi_W + A_N\phi_N + A_S\phi_S + b_\phi \tag{9}$$

where

$$\begin{aligned} A_W &= D_w + C_w U_w^+ \\ A_E &= D_e - C_e U_e^- \\ A_S &= D_s + C_s V_s^+ \\ A_N &= D_n - C_n V_n^- \\ A_P &= A_E + A_W + A_N + A_S - S_\phi^P \Delta V \\ b_\phi &= S_\phi^C \Delta V + S_\phi^b \end{aligned} \tag{10}$$

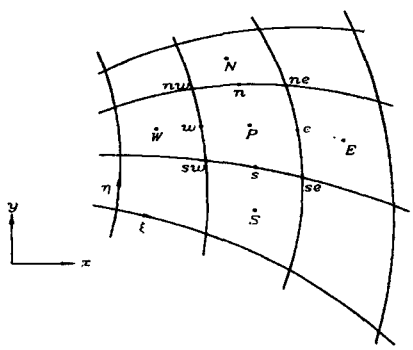

Fig. 1 A typical control volume

and S_ϕ^C, S_ϕ^P are the linearized source terms.

The details of implementation of the higher-order bounded schemes will be outlined in the following chapter.

3. Higher-order bounded schemes

The current high-order bounded schemes are based on the variable normalization by Leonard[6] and the convection boundedness criterion by Gaskell and Lau[5]. Consider, without loss of generality, the west face of control volume. We introduce a normalized variable such that

$$\hat{\phi} = \frac{\phi - \phi_U}{\phi_D - \phi_U} \tag{11}$$

where the subscripts U and D denote the upstream and the downstream locations. Eq.(11) can be rewritten in terms of nodal point values

$$\hat{\phi} = \frac{\phi - \phi_{WW}}{\phi_P - \phi_{WW}} U_w^+ + \frac{\phi - \phi_E}{\phi_W - \phi_E} U_w^- \tag{12}$$

Using the above upwind biased normalized variable, the following four schemes can be written as follows:

Central difference scheme:

$$\begin{aligned} \hat{\phi}_w = {} & [(1 - C_2)\,\hat{\phi}_W + C_2]U_w^+ \\ & + [C_2\,\hat{\phi}_P + (1 - C_2)]U_w^- \end{aligned} \tag{13}$$

First-order upwind scheme:

$$\hat{\phi}_w = \hat{\phi}_W U_w^+ + \hat{\phi}_P U_w^- \tag{14}$$

Second-order upwind scheme:

$$\hat{\phi}_w = (1 + C_1)\,\hat{\phi}_W U_w^+ + (1 + C_3)\,\hat{\phi}_P U_w^- \tag{15}$$

QUICK scheme:

$$\begin{aligned} \hat{\phi}_w = {} & \left[(1 + C_1)(1 - C_2)\,\hat{\phi}_W \right. \\ & \left. + C_2\left(1 - \frac{C_1(1 - C_2)}{C_1 + C_2}\right)\right]U_w^+ \\ & + \left[C_2(1 + C_3)\,\hat{\phi}_P + \right. \\ & \left. (1 - C_2)\left(1 - \frac{C_2 C_3}{1 - C_2 + C_3}\right)\right]U_w^- \end{aligned} \tag{16}$$

where

$$\begin{aligned} C_1 &= \frac{\Delta X_W}{\Delta X_W + \Delta X_{WW}}, \quad C_2 = \frac{\Delta X_W}{\Delta X_W + \Delta X_P} \\ C_3 &= \frac{\Delta X_W}{\Delta X_P + \Delta X_E} \end{aligned} \tag{17}$$

are the geometric interpolation factors defined in terms of the size of control volume cell. For example, ΔX_P is the size of control volume around the calculation point P and is defined as

$$\Delta X_P = \overline{wP} + \overline{Pe} \tag{18}$$

The normalized diagrams for these well-known schemes($U_w > 0$) are shown in Fig.2.

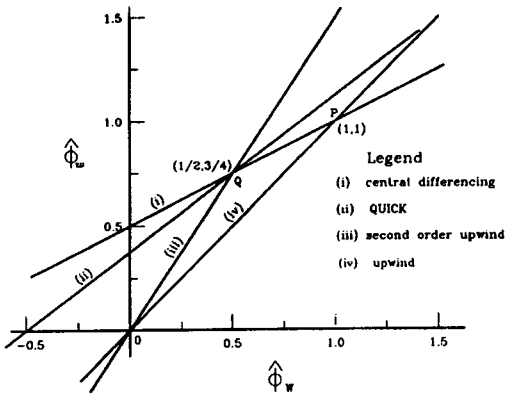

Fig. 2 The normalized variable diagram for various well-known schemes

Gaskell and Lau[5] formulated following convection boundedness criterion. Define a continuous increasing function or union of piecewise continuous increasing function F relating the modelled normalized face value $\hat{\phi}_w$ to the normalized upstream nodal value $\hat{\phi}_W$ ($U_w > 0$), that is $\hat{\phi}_w = F(\hat{\phi}_W)$. Then a finite difference approximation to $\hat{\phi}_w$ is bounded if

(i) for $0 \le \hat{\phi}_W \le 1$, F is bounded below by the function $\hat{\phi}_w = \hat{\phi}_W$ and above by unity and passes through the points(0,0) and(1,1);

(ii) for $\hat{\phi}_W < 0$, $\hat{\phi}_W > 1$, F is equal to $\hat{\phi}_W$.

The convection boundedness criterion is a necessary and sufficient condition for achieving computed boundedness if only three neighbouring upstream nodal values are used to approximate the face values. The diagrammatic representation of the convection boundedness criterion is shown in Fig.3.

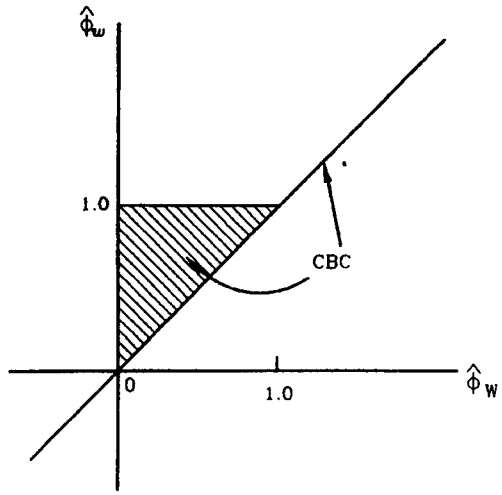

Fig. 3 Diagrammatic representation of the convection boundedness criterion

According to Leonard[6], for any(in general non-linear) characteristics in the normalized variable diagram(Fig.2),

(i) passing through Q is necessary and sufficient for second-order accuracy

(ii) passing through Q with a slope of 0.75(for a uniform grid) is necessary and sufficient for third-order accuracy.

The horizontal and vertical coordinates of point Q in the normalized variable diagram and the scope of the characteristics at the point Q for preserving the third order accuracy for a non-uniform grid can be obtained by a simple algebra using Eqs.(13)-(16).

$$\begin{aligned} X_Q &= \frac{C_2}{C_1 + C_2} U_w^+ + \frac{1 - C_2}{1 - C_2 + C_3} U_w^- \\ Y_Q &= \frac{C_2(1 + C_1)}{C_1 + C_2} U_w^+ \\ &\quad + \frac{(1 - C_2)(1 + C_3)}{1 - C_2 + C_3} U_w^- \\ S_Q &= (1 + C_1)(1 - C_2) U_w^+ + C_2(1 + C_3) U_w^- \end{aligned} \tag{19}$$

For a uniform grid, $X_Q = 0.5$, $Y_Q = 0.75$ and $S_Q = 0.75$. Following the above criteria by Gaskell and Lau[5] and by Leonard[6], one may

choose several bounded characteristics in the normalized variable diagram whose order of accuracy is determined by the shape of the characteristics. Followings are four simple possibilities which ensure the second or third-order accuracy.

The SOUCUP scheme

The SOUCUP scheme[8] employs union of piecewise linear characteristics passing through the points, O, Q and P in the normalized variable diagram

$$\begin{aligned} \hat{\phi}_w &= a_w + b_w \hat{\phi}_C & 0 \le \hat{\phi}_C \le X_Q \\ &= c_w + d_w \hat{\phi}_C & X_Q \le \hat{\phi}_C \le 1 \\ &= \hat{\phi}_C & \textit{otherwise} \end{aligned} \tag{20}$$

where

$$\begin{aligned} a_w &= 0 \\ b_w &= Y_Q / X_Q \\ c_w &= (Y_Q - X_Q)/(1 - X_Q) \\ d_w &= (1 - Y_Q)/(1 - X_Q) \end{aligned} \tag{21}$$

and

$$\hat{\phi}_C = \hat{\phi}_W U_w^+ + \hat{\phi}_P U_w^- \tag{22}$$

Eq.(19) indicates that above constants vary according to the flow direction at the same cell face when the numerical grids are non-uniform. The SOUCUP scheme is composite of second-order upwind, central differencing and first-order upwind scheme. We see that the SOUCUP scheme is second-order accurate according to the criteria by Leonard[6]. As will be shown later, the way of implementation of this scheme in the present study is slightly different from that reported in Zhu and Rodi[8].

The HLPA scheme

In this scheme, the normalized face value is approximated by a combination of linear and parabolic characteristics passing through the points, O, Q and P in the normalized variable diagram

$$\begin{aligned} \hat{\phi}_w &= a_w + b_w \hat{\phi}_C + c_w \hat{\phi}_C^2 & 0 \le \hat{\phi}_C \le 1 \\ &= \hat{\phi}_C & \textit{otherwise} \end{aligned} \tag{23}$$

where

$$\begin{aligned} a_w &= 0 \\ b_w &= (Y_Q - X_Q^2)/(X_Q - X_Q^2) \\ c_w &= (X_Q - Y_Q)/(X_Q - X_Q^2) \end{aligned} \tag{24}$$

Zhu[9] developed this scheme on the assumption of uniform grid(in this case, $a_w = 0$, $b_w = 2$, $c_w = -1$). The original scheme is further extended for use on the non-uniform grid in the present study. This scheme is second- order accurate.

The SMARTER scheme

The order of accuracy of the scheme may be increased to the third order if one introduces a characteristic curve in the normalized variable diagram whose slope at the intersection point Q is the same as that of the third-order accurate QUICK scheme. Such a scheme has been developed by Shin and Choi[10] using following characteristics in the normalized variable diagram

$$\begin{aligned} \hat{\phi}_w &= a_w + b_w \hat{\phi}_C + c_w \hat{\phi}_C^2 \\ &\quad + d_w \hat{\phi}_C^3 & 0 \le \hat{\phi}_C \le 1 \\ &= \hat{\phi}_C & \textit{otherwise} \end{aligned} \tag{25}$$

where

$$\begin{aligned} a_w &= 0 \\ b_w &= \frac{X_Q^4 + S_Q(X_Q^3 - X_Q^2) + Y_Q(2X_Q - 3X_Q^2)}{(X_Q - X_Q^2)^2} \\ c_w &= \frac{-2X_Q^3 + S_Q(X_Q - X_Q^3) + Y_Q(3X_Q^2 - 1)}{(X_Q - X_Q^2)^2} \\ d_w &= \frac{X_Q^2 + S_Q(X_Q^2 - X_Q) + Y_Q(1 - 2X_Q)}{(X_Q - X_Q^2)^2} \end{aligned} \tag{26}$$

The COPLA scheme

Another possible way of devising a third-order accurate scheme is to employ a composite of piecewise linear characteristics in which the QUICK scheme is employed in a range of $0.5X_Q \le \hat{\phi}_C \le 1.5X_Q$. This scheme is similar to the SMART scheme[5], but is free of convergence oscillation. Such a scheme was

proposed by Choi et al.[11] employing following characteristics in the normalized variable

$$\begin{aligned}\hat{\phi}_w &= a_w + b_w\hat{\phi}_C \quad && 0 \le \hat{\phi}_C \le 0.5X_Q \\ &= c_w + d_w\hat{\phi}_C \quad && 0.5X_Q \le \hat{\phi}_C \le 1.5X_Q \\ &= e_w + f_w\hat{\phi}_C \quad && 1.5X_Q \le \hat{\phi}_C \le 1 \\ &= \hat{\phi}_C && \textit{otherwise}\end{aligned} \tag{27}$$

where

$$\begin{aligned}a_w &= 0 \\ b_w &= (2Y_Q - S_Q X_Q)/X_Q \\ c_w &= Y_Q - S_Q X_Q \\ d_w &= S_Q \\ e_w &= (3X_Q - 2Y_Q - S_Q X_Q)/(3X_Q - 2) \\ f_w &= (2Y_Q + S_Q X_Q - 2)/(3X_Q - 2)\end{aligned} \tag{28}$$

The normalized variable diagrams for the higher-order bounded schemes considered in the present study are given in Fig.4.

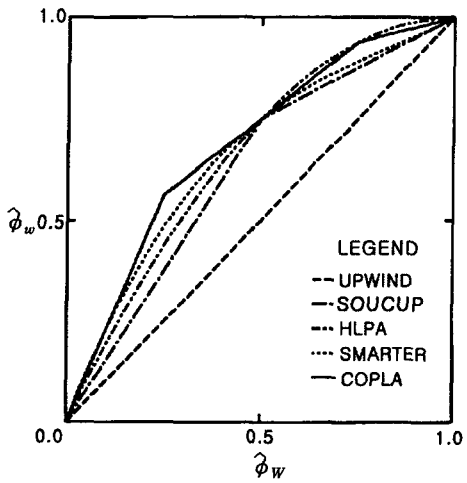

Fig. 4 The normalized variable diagram for bounded schemes

It is worthwhile mentioning here that the present bounded schemes are very similar to the shock capturing schemes based on the Total Variational Diminishing flux limiters (TVD), which are widely used in the compressible flow calculations. The SOUCUP scheme is similar to the MINMOD(MINimum MODulus) scheme of Roe[12] and the HLPA scheme is similar to the CLAM(Curved Line Advection Method) scheme of Van Leer[13].

The implementation of the higher-order bounded schemes is quite simple. We note that the forementioned four bounded schemes employ very similar forms of characteristics in the normalized variable diagram. They differ only in the order of the characteristics and the values of the constants. Therefore, it suffices to present the implementation of one scheme here, for example, the HLPA scheme. In the present work, the higher-order schemes are implemented in a deferred correction way proposed by Khosla and Rubin[14].

Eq.(23) can be expressed in terms of the unnormalized variable

$$\begin{aligned}\phi_w = &\{\phi_W + (\phi_P - \phi_{WW})[a_w^+ + (b_w^+ - 1)\left(\frac{\phi_W - \phi_{WW}}{\phi_P - \phi_{WW}}\right) + c_w^+\left(\frac{\phi_W - \phi_{WW}}{\phi_P - \phi_{WW}}\right)^2]\}U_w^+ \\ &+\{\phi_P + (\phi_W - \phi_E)[a_w^+ + (b_w^- - 1)\left(\frac{\phi_P - \phi_E}{\phi_W - \phi_E}\right) + c_w^-\left(\frac{\phi_P - \phi_E}{\phi_W - \phi_E}\right)^2]\}U_w^-\end{aligned} \tag{29}$$

Given the switch factors

$$\begin{aligned}\text{for } U_w > 0: \quad a_w^+ &= 1 \quad \text{if } |\phi_P - 2\phi_W + \phi_{WW}| < |\phi_P - \phi_{WW}| \\ a_w^+ &= 0 \quad \textit{otherwise}\end{aligned} \tag{30}$$

$$\begin{aligned}\text{for } U_w < 0: \quad a_w^- &= 1 \quad \text{if } |\phi_W - 2\phi_P + \phi_E| < |\phi_W - \phi_E| \\ a_w^- &= 0 \quad \textit{otherwise}\end{aligned} \tag{31}$$

the unnormalized form of Eq.(29) can be rewritten as

$$\phi_w = U_w^+\phi_W + U_w^-\phi_P + \Delta\phi_w \tag{32}$$

where

$$\begin{aligned}\Delta\phi_w = &\; U_w^+ a_w^+(\phi_P - \phi_{WW})[a_w^+ + (b_w^+ - 1)\left(\frac{\phi_W - \phi_{WW}}{\phi_P - \phi_{WW}}\right) + c_w^+\left(\frac{\phi_W - \phi_{WW}}{\phi_P - \phi_{WW}}\right)^2] \\ &+ U_w^- a_w^-(\phi_W - \phi_E)[a_w^+ + (b_w^- - 1)\left(\frac{\phi_P - \phi_E}{\phi_W - \phi_E}\right) + c_w^-\left(\frac{\phi_P - \phi_E}{\phi_W - \phi_E}\right)^2]\end{aligned} \tag{33}$$

After the evaluation of the additional term, the implementation of this scheme is the same as that of the first-order upwind scheme. In the

SOUCUP and LAPPA schemes, the constants are switched according to the value of $\hat{\phi}_C$ at the same cell face and for the same flow direction.

4. Applications to test problems

All the higher-order bounded schemes described in the previous chapter are implemented in a general purpose computer code designed to solve fluid flow and heat transfer in complex geometries. The computer code uses a non-staggered grid arrangement and the SIMPLE[1] algorithm for pressure-velocity coupling. The momentum interpolation practice by Rhie and Chow[15] is employed for calculating the cell-face mass fluxes to avoid the pressure oscillation.

The test problems include: (1)pure convection of a scalar variable in three different situations, (2)laminar flow in a lid-driven cavity with and without inclination. The computed results are compared with the analytic solutions, the avaliable benchmark solutions and the results by the lower-order HYBRID scheme and by the higher-order unbounded QUICK scheme.

4.1 Pure convection of a scalar variable

In what follows, we present the results of three linear problems involving purely convective transport of scalar tracers containing discontinuities by prescribed velocity fields. They are: (1)pure convection of a scalar step by a uniform velocity field, (2)pure convection of a scalar step by a rotational velocity field, (3)pure convection of a box-shaped scalar step by a uniform velocity field. These simple yet stringent test cases were extensively used in the literature to examine the performance of the convection schemes.

The flow configuration for Case 1 is shown in Fig.5. Calculations are performed for two different flow angles, $\theta=45^\circ$ and $\theta=26.6^\circ$, employing 22×22 uniform grids. Fig.6 shows the predicted profiles along the centerline by different convection schemes. It can be seen that the HYBRID scheme results in a very diffusive profiles at both angles. Both accuracy and boundedness are achieved by the bounded schemes. The sharp gradient is fairly well resolved without introducing the spurious overshoots and undershoots. We can observe that the SOUCUP scheme is relatively more diffusive than the other three bounded schemes. The overall solution behaviors are not much influenced by the flow angle. The QUICK scheme also fairly well resolves the steep gradient, but exhibits oscillatory behaviors. This oscillatory solution behaviour is not reduced with the grid refinement and is a little sensitive to the orientation of the flow field. The magnitude of undershoot is more pronounced at a smaller flow angle($\theta=26.6^\circ$).

In the second test case(Case 2) shown in Fig.7, a scalar profile with a discontinuity at x=-0.5 is convected counter-clockwise from the inlet plane(x<0, y=0) to the outlet plane(x>0, y=0) by a rotational velocity field given by

$$u=-2y(1-x^2), \quad v=2x(1-y^2) \tag{34}$$

Calculations are performed with 42×22 and 82×42 uniform grids. Fig.8 shows the computed profiles along the horizontal exit plane ($0\le x\le1$, $y=0$) for each grid. The general performances of each convection scheme in this case are nearly the same as those in the previous case, except the QUICK scheme exhibits relatively large overshoots in this case.

As a third test problem of pure convection (Case 3), we consider a box-shaped profile shown in Fig.9 which is generated by imposing a step profile along the bottom and left-hand walls of the square solution domain. Calculations are performed with two different meshes, 22×22 and 42×42. The predicted profiles along the vertical centerline ($x=0.5$, $0\le y\le1$) are shown in Fig.10. We can observe that the solutions by the HYBRID scheme are very diffusive, even the grids are increased by a factor of two. The QUICK scheme results in severe overshoots when the grid is coarse(22×22), but shows relatively low undershoots. The bounded schemes fairly well resolve the steep gradient on either side of the peaked profile. The SOUCUP scheme is more diffusive than the other bounded schemes again, but is much better than the HYBRID scheme.

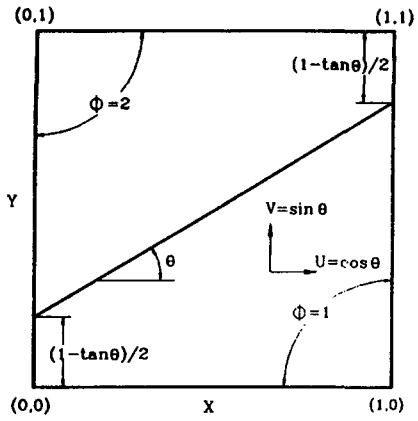

Fig. 5 Case 1: Pure convection of a scalar step by a uniform velocity field

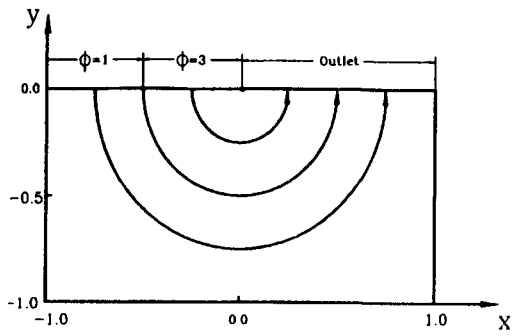

Fig. 7 Case 2: Pure convection of a scalar step by a rotating velocity field

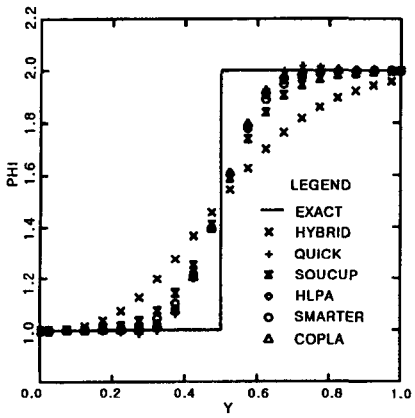

(a) θ =45°

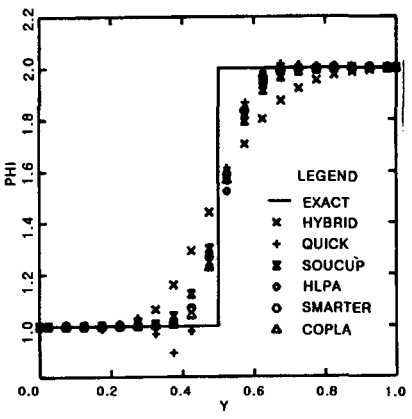

(b) θ =26.6°

Fig. 6 ϕ-profiles along the centerline

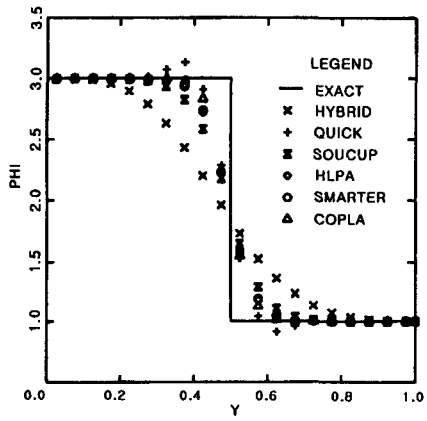

(a) 42×22 grid

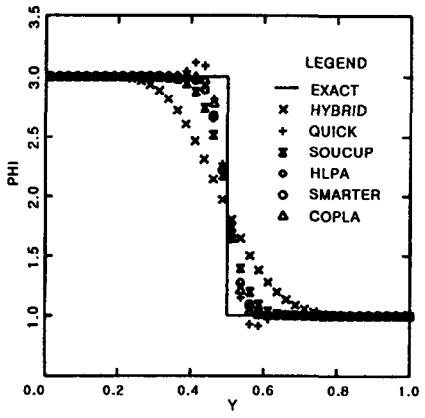

(b) 82×22 grid

Fig. 8 ϕ-profiles at outlet

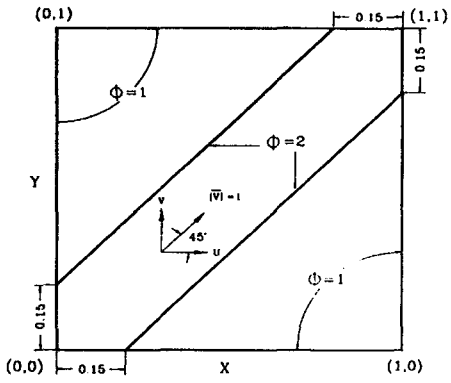

Fig. 9 Case 3: Pure convection of a box-shaped scalar step by a uniform velocity field

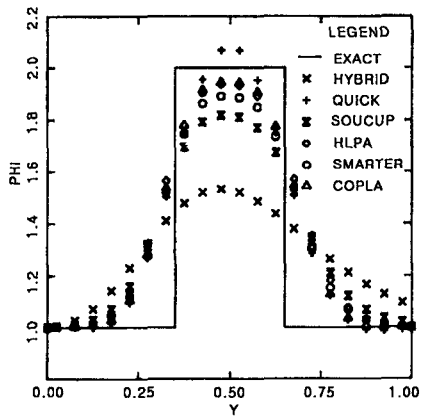

(a) 22×22 grid

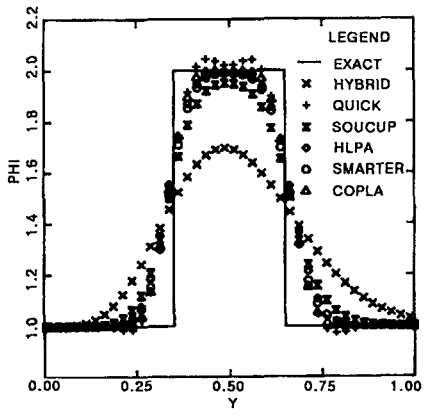

(b) 42×42 grid

Fig. 10 ϕ-profiles along the centerline

4.2. Laminar flow in a lid-driven cavity with and without inclination

Laminar flow in a lid-driven square cavity, schematically shown in Fig.11, is considered as an example of non-linear problems which are of practical interest. Two cases with different inclinations(β =90° , β =45°) are considered to examine the grid non-orthogonality effect on the solution behaviors. At present reliable benchmark solutions are available for both cases. Calculations are performed for Reynolds number of 1000 employing 42×42 uniform grid. The computed results are compared with the benchmark solutions by Ghia et al,[16](β =90°) and by Demirdzic et al.[17](β =45°).

The computed U-velocity profiles along the vertical centerline for both cases are presented in Fig.12. For these recirculating type flow calculations, the QUICK scheme results in the most accurate solution. The results by the HYBRID scheme are far from the benchmark solution. The HLPA, SMARTER and COPLA schemes work similarly, but are slightly less accurate than the QUICK scheme. The SOUCUP scheme is again more diffusive than the other three bounded schemes. The general solution behaviors among the different convection schemes are not altered with the change of the grid non-orthogonality.

5. Conclusions

A comparison has been made of four recently developed higher-order bounded schemes SOUCUP, HLPA, SMARTER and COPLA together with HYBRID and QUICK schemes. The following are some findings from the numerical experiments conducted in the present study.

(1) All the bounded schemes resolve the boundedness problem retaining the accuracy of the higher-order scheme.

(2) The bounded schemes are simple to implement and computationally cost effective.

(3) The SOUCUP scheme is relatively more diffusive than the HLPA, SMARTER and COPLA chemes, but shows a better convergence rate.

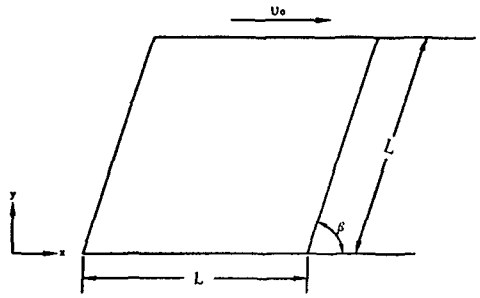

Fig. 11 Larminar flow in a lid-driven cavity

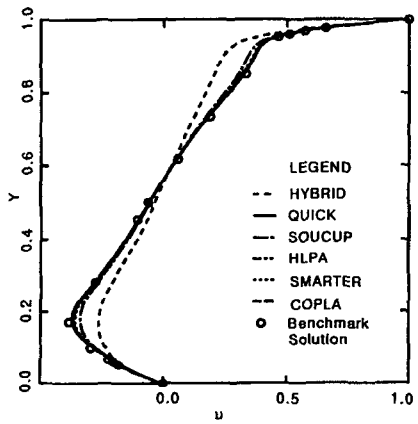

(a) β=90°

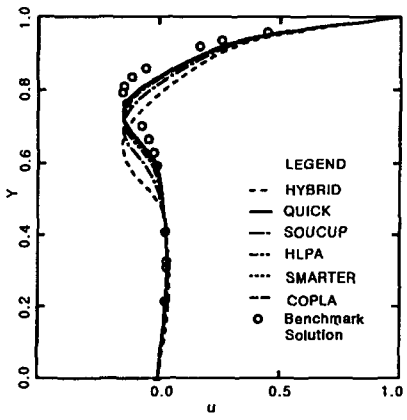

(b) β=45°

Fig. 12 Centerline velocity profiles

(4) The HLPA, SMARTER and COPLA schemes show nearly the same solution behaviors both in accuracy and in convergence. The implementation of SMARTER and COPLA schemes is slightly more complicated than that of the HLPA or SOUCUP schemes.

References

[1] Patankar, S. V., Numerical Heat Transfer and Fluid Flow (McGraw-Hill, New York, 1980).

[2] Leonard, B. P., " A stable and accurate convective modelling procedure based on quadratic interpolation," Comput. Methods Appl. Mech. Engrg. 19 (1979), P.59-98.

[3] Warming, R. F. and Beam, R. M., " Upwind second order difference schemes and applications in aerodynamic flows," AIAA J. 14 (1976), P.1241-1249.

[4] Raithby, G. D., " Skew upstream differencing schemes for problem involving fluid flow," Comput. Methods Appl Mech. Engrg. 9 (1979), P.153-164.

[5] Gaskell, P. H. and Lau, A. K. C., " Curvature-compensated convective transport: SMART, a new boundedness preserving transport algorithm," Internat. J. Numer. Methods Fluids 8(1988), P.617-641.

[6] Leonard, B. P., " Simple high-accuracy resolution program for convective modelling of discontinuities," Internat J. Numer. Methods Fluids 8 (1988), P.1291-1318

[7] Zhu, J., " On the higher-order bounded discretization schemes for finite volume computations of incompressible flows," Comput. Methods Appl. Mech. Engrg. 98 (1992), P.345-360.

[8] Zhu, J. and Rodi, W., " A low dispersion and bounded convection scheme," Comput. Methods Appl. Mech. Engrg. 92 (1991), P.225-232.

[9] Zhu, J., " A low-diffusive and oscillation-free convection scheme," Comm. Appl. Numer. Methods 7 (1991), P.225-232.

[10] Shin, J. K. and Choi, Y. D., " Study on the improvement of the convective differencing scheme for the high-accuracy and stable resolution of the numerical solution," Trans. KSME 16(6) (1992), P.1179-1194.

[11] Choi, S. K., Nam, H. Y. and Cho, M., " Evaluation of a higher-order bounded convection scheme: three dimensional numerical experiments," Numer. Heat Transfer, part B, 28 (1995), P.23-38.

[12] Roe, P. L., " Characteristic-based schemes for the Euler equations," in: M Van Dyke et al., eds., Annual Reviews of Fluid Mechanics, 18 (Annual Reviews CA, 1986), P.337.

[13] Van Leer, B., " Towards the ultimate conservative difference scheme Ⅱ. Monotonicity and conservation combined in a second order scheme," J. Comput. Phys. 14 (1974), P.361-370.

[14] Khosla, P. K. and Rubin, S. G., " A diagonally dominant second order accurate implicit scheme," Comput. Fluids 2 (1974), P.207-209.

[15] Rhie, C. M. and Chow, W. L., " Numerical study of the turbulent flow past an airfoil with trailing edge separation," AIAA J. 21 (1983), P.1525-1532.

[16] Ghia, U., Ghia, K. N. and Shin, C. T., " High-Re solutions for incompressible flow using the Navier-Stokes equations and a multigrid method," J. Comput. Physics 48 (1982), P.387-411.

[17] Demirdzic, L., Lilek, Z. and Peric, M., " Fluid flow and heat transfer test problems for non-orthogonal grids: bench-mark solutions," Internat. J. Numer. Methods Fluids 15 (1992), P.329-354.